

Xp11.2 Translocation Renal Cell Carcinoma With Very Aggressive Course in Five Adults

Paul N. Meyer, MD, PhD,¹ Joseph I. Clark, MD,² Robert C. Flanigan, MD,³ and Maria M. Picken, MD, PhD¹

Key Words: Translocation; Renal; Carcinoma; TFE3; TFEB; Adult; Aggressive; Clinical

DOI: 10.1309/LR5G1VMXPY3G0CUK

Abstract

Renal cell carcinomas associated with Xp11.2 translocations (TFE3 gene fusions) are rare tumors predominantly reported in children. We studied 5 cases of translocation carcinoma in adult patients, 18 years or older (mean age, 32.6 years). Tumors were examined histologically, immunohistochemically, and electron microscopically and correlated with the clinical picture. Most tumors showed solid sheets of clear to eosinophilic cells with rich vasculature and foci of papillary or pseudopapillary architecture. All cases showed strong nuclear positivity for TFE3. Vimentin and CD10 were positive in the cytoplasm. A panel of cytokeratin antibodies, smooth muscle actin, CD45, HMB45, and calretinin were negative. Patients had nonspecific initial complaints and were diagnosed with advanced disease, most with distant metastases. Various treatments met with minimal success. Unlike pediatric patients, the adult patients followed a rapidly terminal course, with a mean survival of 18 months after diagnosis (range, 10-24 months).

Based on the cytoplasmic appearance of tumor cells in H&E-stained sections, renal cell carcinomas (RCCs) originally were categorized as 1 of 3 entities: clear cell carcinoma, granular cell carcinoma, or mixed clear and granular cell carcinoma. With the increased use of new methods for examining tumors, the classification of RCCs has expanded and evolved^{1,2} and currently includes clear cell (conventional), papillary, chromophobe, collecting duct, and the recently recognized mucinous tubular and spindle cell carcinoma. A number of new entities with characteristically eosinophilic cytoplasm have emerged from the granular cell category, including chromophobe carcinoma, oncocytoma, and epithelioid angiomyolipoma.

Despite these changes in classification, 75% of epithelial renal tumors are still diagnosed as clear cell (conventional) carcinoma. The likely explanation for this high rate of diagnosis is that RCC, clear cell type, is heterogeneous and contains several entities that are not discernible with currently applied methods. In support of this explanation, translocations involving the Xp11.2 locus were recently detected in a number of RCCs previously classified as clear cell type.¹⁻³

Translocations involving Xp11.2 have been demonstrated in alveolar soft part sarcoma.^{3,4} The gene of interest, located at Xp11.2, is *TFE3*, a member of the microphthalmia transcription factor (MiTF) family.⁵ Members of this family of proteins code for basic-helix-loop-helix leucine-zipper transcription factors that bind DNA as homodimers or heterodimers.^{5,6} Other members of this family include *TFEB* and *TFEC*, at least one of which (*TFEB*) is also involved in other recently recognized RCCs.⁷

In RCCs, fusion of *TFE3* with several different genes can occur, depending on the exact translocation. Currently, 4 distinct

recipient genes have been identified: *PRCC* (1q21), *ASPL* (17q25), *PSF* (1p34), and *NonO* (Xq12).^{4,8-10}

RCCs associated with Xp11.2 translocations are rare and predominantly reported in children.¹ RCCs resulting from these translocations typically have papillary architecture and are composed of cells with voluminous clear or eosinophilic cytoplasm. Although little is known of the clinical course of these tumors, they are believed to be indolent, even when diagnosed at advanced stages.¹

We summarize the histologic and clinical findings in 5 adult cases of translocation RCC with immunohistochemical evidence of TFE3 overexpression. All patients had nonspecific disease manifestations followed by a rapidly terminal disease course.

Report of Cases

Case 1

A 30-year-old white man with flank pain and hematuria had a medical history significant only for gastric ulcers at 18 years, a family history significant only for a maternal grandmother with bladder cancer, and a social history significant for a 10-pack-year history of smoking and social use of alcohol. He had no history of hazardous exposures or chemotherapy. A computed tomography (CT) scan demonstrated a mass in the right flank extending through the renal vein and into the inferior vena cava (IVC). The patient underwent a right radical nephrectomy and IVC thrombectomy. The gross and microscopic appearance of the tumor is described in the "Results" section.

Approximately 5 months after nephrectomy, an abdominal CT scan revealed multiple 5-mm nodules between the liver and abdominal wall, which a biopsy revealed to be metastatic RCC. High-dose interleukin (IL)-2 therapy was started 6 months after the nephrectomy, and the patient completed 1 full course. Disease progression continued despite IL-2 treatment, and the patient received various investigational agents, including PS341 (proteasome inhibitor), combination chemotherapy with gemcitabine plus capecitabine, and NK92 cell infusion therapy (phase 1 trial). None of these therapies proved beneficial, and the patient died approximately 20 months after nephrectomy.

Case 2

An 18-year-old Hispanic man with abdominal pain had no significant medical history, no family history of cancer, and no history of hazardous exposures or chemotherapy, and he did not use tobacco or alcohol. Physical examination revealed a palpable abdominal mass. A CT scan confirmed a large right kidney tumor measuring 14.0 × 10.7 × 9.0 cm, along with an adjacent retroperitoneal mass measuring 14.0 × 9.6 × 5.7 cm

with encasement of the superior mesenteric artery and other mesenteric vessels. Metastases were identified in the right 12th rib, right acetabulum, left acetabulum, and both lungs. Because of the vascular encasement, surgery was not considered feasible. A needle biopsy of the renal mass yielded nondiagnostic fibrotic tissue.

Approximately 3 months after initial examination, right leg weakness developed. A thoracic laminectomy at T11 was performed to remove a metastatic deposit causing impending spinal cord compression. The initial laminectomy was followed by a video-assisted thoracoscopic surgery with talc pleurodesis to control a malignant pleural effusion.

After the initial surgeries, the patient received palliative radiation to symptomatic bony metastases followed by chemotherapy with gemcitabine and capecitabine. He received only 1.5 cycles of this therapy and was readmitted with spinal cord compression due to recurrence of thoracic metastasis and requiring surgical decompression. He was discharged to hospice care 10 months after diagnosis and was, unfortunately, lost to follow-up. Microscopic descriptions of the metastases are given in the "Results" section.

Case 3

A 39-year-old white man noticed easy fatigability and increased blood pressure (190/90 mm Hg), followed by gross hematuria. His medical history was significant only for a left knee repair, and he had no family history of cancer and no history of hazardous exposures or chemotherapy. His social history was significant for a 17-pack-year history of smoking and social use of alcohol. A CT scan demonstrated a 7.5 × 6.5 × 5-cm mass in the left kidney and a 9-mm mass in the lower lobe of the right lung. The patient underwent radical left nephrectomy and resection of the right lower lung lobe. Gross and microscopic descriptions of the tumor are given in the "Results" section.

The patient completed 2 cycles of high-dose IL-2 therapy. Approximately 2 months later, he sought care because of word finding difficulty and expressive aphasia. Magnetic resonance imaging revealed a 3-cm lesion in the temporal horn of the left lateral ventricle, which was resected. Subsequently, the patient received whole-brain radiotherapy, 37.5 Gy, in 15 sessions, followed several months later by 22 Gy of stereotactic radiotherapy to a 5-mm nodule in the left tentorium. The patient received combination chemotherapy with gemcitabine and capecitabine 13 months after diagnosis without success. Further therapy consisted of cryoablation and radiosurgery of metastatic deposits. At the time of this writing, the patient was 24 months postdiagnosis.

Case 4

A 35-year-old white man with left pleuritic chest pain radiating to his back, dark-colored urine, and fatigue had a

medical history significant for type 2 diabetes mellitus of 7 years, for which he was taking oral hypoglycemic medication (his only constant medication). The patient's family history consisted of a maternal aunt with Hodgkin disease but no other malignancies. His social history was significant for "binge drinking" of alcohol, use of cocaine for 5 years, and use of marijuana for 18 years. A recent HIV test was negative. A CT scan of his chest and abdomen revealed bilateral lung nodules, the largest measuring 2.1 cm, and an approximately 11-cm mass in the superior pole of the left kidney. The patient underwent a radical left nephrectomy. Gross and microscopic descriptions of the tumor are given in the "Results" section.

Approximately 1 month after nephrectomy, the patient sought care because of abdominal pain, nausea, and vomiting. A CT scan demonstrated numerous nodules in the liver consistent with metastases, the largest measuring 6.9 × 5.5 cm. A CT scan of the chest showed extensive mediastinal adenopathy, the largest node measuring 4.9 × 2.9 cm. No axillary adenopathy was identified. The patient did not want IL-2 therapy and was considered a poor candidate for interferon alfa therapy. Combination chemotherapy with gemcitabine plus capecitabine was started, and he was lost to follow-up 6 months after diagnosis.

Case 5

A 41-year-old white man with dizziness, weakness, polyuria, polydipsia, and a 40-pound weight loss during 6 months had a medical history significant only for borderline diabetes mellitus. The patient's family history was significant for a brother with end-stage renal disease (nonneoplastic) and a maternal grandmother with a "brain tumor." The social history was significant for 20-pack-year tobacco use. A CT scan revealed a large right renal mass (11.7 × 13.2 × 14 cm) with additional masses in the middle anterior part of the abdomen adjacent to the colon (4.4 × 7.5 cm) and in the distal transverse colon (3.2 cm). The patient underwent a right radical nephrectomy and segmental transverse colon resection. Gross and microscopic descriptions of the tumor are presented in the "Results" section.

Approximately 1 month after surgery, a CT scan revealed bilateral nodules in the lungs, each approximately 5 mm. He elected observation of the lung nodules without surgical or medical treatment and was subsequently lost to follow-up.

Materials and Methods

Formalin-fixed, paraffin-embedded tissue sections measuring 5 μm in thickness were stained with H&E for light microscopic analysis. Immunohistochemical staining was performed using a Ventana Benchmark automated stainer (Ventana, Tucson, AZ) using the avidin-biotin method.

Antigen retrieval was performed using protease 1 digestion (AE1, AE3, cytokeratin [CK]7, ker34βE12, pankeratin, and vimentin), EDTA steam-mediated retrieval (calretinin, CD10, collagen IV, and HMB45), or Borg decloaking (TFE3, Biocare Medical, Concord, CA).

The antibodies, vendors, and dilutions used were as follows: AE1, AE3, calretinin, CD10, CK7, collagen IV, HMB45, ker34βE12, pankeratin, and vimentin (Ventana, prediluted); leukocyte common antigen (LCA; Biocare, prediluted); smooth muscle actin (SMA; Zymed Laboratories [Invitrogen], Carlsbad, CA, prediluted); and TFE3 (dilution 1:1,600; Santa Cruz Biotechnology, Santa Cruz, CA). In view of the differential diagnoses (which included RCC of the clear cell type, translocation carcinomas, and epithelioid angiomyolipoma) the following antibodies were applied: CD10, vimentin, TFE3, TFEB, SMA, and HMB45. Considering the positivity for TFE3, several cytokeratin markers were also added: AE1, AE3, CK7, and ker34βE12. Staining for LCA was used to confirm the presence of a lymphocytic infiltrate within some tumors. Finally, stains for collagen IV and calretinin were used to examine the basement membrane–like hyaline granules or possible mesothelial derivation in some tumors.

Electron microscopy was performed as previously described.¹¹

Results

Clinical Findings

The patients in **Table 1** ranged in age from 18 to 41 years, with a mean age of 32.6 years. Initial complaints were nonspecific, and included fatigue and hematuria. The medical history was not significant in any of the cases. Four patients had distant metastases at diagnosis. Four of the patients underwent nephrectomy as part of the treatment plan, allowing examination of the primary tumor.

Gross Findings

The lower pole of the kidney in case 1 contained a circumscribed light tan nodule measuring 11.5 × 10.2 × 9.0 cm with focal cystic areas of hemorrhage and necrosis, which was surrounded by a grossly intact capsule. The renal vein and a segment of the IVC were occluded by tumor thrombus. Of 7 lymph nodes examined, 2 contained tumor. Based on these findings, the case was staged as T3b N2 Mx.

Patient 2 did not undergo a nephrectomy, and only biopsies of a perispinal mass and pulmonary nodules were available for examination. Based on the distant metastases and CT scan results, the case was staged as T4 Nx M1.

The left kidney in case 3 showed a 5.5-cm light tan mass in the central hilar region contained within the capsule and

Table 1
Clinical Information for Five Patients With Renal Cell Carcinoma Associated With Xp11.2*

Case No./ Sex/Age (y)	Race/ Ethnicity	Symptoms	Tumor Size (cm) and TNM	Initial Location	Metastases	Treatment	Follow-up (mo After Diagnosis)
1/M/30	White	Flank pain; hematuria	11.5 × 10.2 × 9.0; T3b N2 Mx	Lower pole R kidney extending through renal vein into IVC	Perihepatic within 5 mo	Nephrectomy; IL-2; chemo; experimental	Death (20)
2/M/18	Hispanic	Abdominal pain; palpable mass	14 × 10.7 × 9 and 14 × 9.6 × 5.7; T4 Nx M1	R flank; thoracic spine; pelvis; both lungs	Thoracic recurrence	Laminectomy; pleurodesis; radiation; chemo; decompression	Hospice (10)
3/M/39	White	Fatigue; increased BP; hematuria	5.5 diameter; T1b N0 M1	L kidney; R lung	Brain (L lateral ventricle, temporal horn)	Nephrectomy; lung resection; IL-2; brain resection; brain radiation; chemo; cryo-ablation; radiosurgery	Alive (24)
4/M/35	White	Lsided pleuritis; fatigue	10 × 7 × 7; T3a N2 M1	Superior pole L kidney; L adrenal; both lungs	Liver	Nephrectomy; chemo	Lost to follow-up (6)
5/M/41	White	Fatigue; polyuria; polydipsia; weight loss	14 × 12 × 11; T2 Nx M1	R kidney; mid abdomen; transverse colon	L lower lung	Nephrectomy; colon resection	Lost to follow-up (3)

BP, blood pressure; IVC, inferior vena cava; IL-2, interleukin 2; chemo, chemotherapy (gemcitabine and capecitabine).

* Age is age at diagnosis; initial tumor size determined by gross (cases 1, 3, and 4) or computed tomography (case 2) measurement; and follow-up is the outcome at the time of writing.

without extension into the perinephric fat. Focal invasion of the calyx was present without invasion of the renal vein. Five perirenal lymph nodes were negative for metastases. Gross analysis of the lung resection revealed 3 foci of tumor, the largest 8 mm in diameter. Based on these findings, the case was staged as T1b N0 M1.

The upper pole of the kidney in case 4 contained a 10 × 7 × 7-cm variegated, partially necrotic nodule with areas of fibrosis and gross extension through the capsule and into the

perihilar fat and adrenal gland (Image 1). The renal vein, pelvis, and ureter were not involved by tumor. Of 3 hilar lymph nodes, 2 contained metastases. Retroperitoneal lymphadenopathy was also present. Based on these findings, the case was staged as T3a N2 M1.

The kidney in case 5 contained a 14 × 12 × 11-cm extensively necrotic mass, with an intact renal capsule. There was no involvement of the renal vessels, ureter, fascia, or adrenal gland. The segment of transverse colon contained

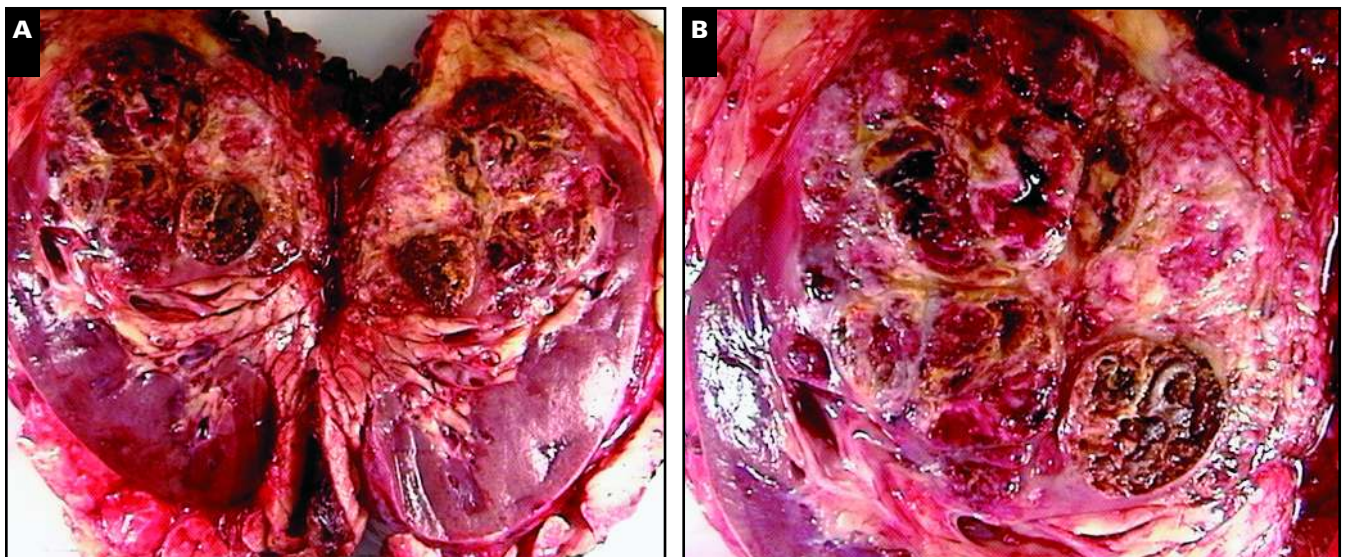


Image 1 (Case 4) Variegated, partially necrotic nodule with areas of fibrosis located in the superior pole of the left kidney, measuring 10 × 7 × 7 cm. The tumor grossly extended through the renal capsule into the perirenal fat and adrenal gland. The renal vein, renal pelvis, and ureter were not involved by tumor. Bisected nephrectomy specimen (A) and the cut surface of the tumor (B) are shown.

a 7 × 7 × 5-cm subserosal mass involving the colonic wall. Based on these findings, the case was staged as T2 Nx M1.

Microscopy

Microscopic examination of the primary and metastatic tumors revealed a mixture of cells with eosinophilic granular and clear cytoplasm **Image 2**, with the tumor in case 5 composed entirely of eosinophilic granular cells. All tumors were composed of a single population of neoplastic epithelial cells; however, the tumor in case 3 contained an admixture of lymphocytes (Image 2B). The amount of cytoplasm ranged from moderate to voluminous. The nuclear grade ranged from 2 to 4 (out of 4) (Image 2). Four tumors showed predominantly solid sheets of cells with rich vasculature **Image 3A** and **Image 3B** and foci of pseudopapillary structures lacking true fibrovascular cores **Image 3C**. Only the tumor in case 1 contained distinct papillary architecture with fibrovascular cores supporting the neoplastic cells **Image 3D**. Focal nodules of tumor cells were also present in most tumors **Image 3E**. Tubule formation was not present in any of the tumors. The original tumor in case 2 could not be examined, but metastatic deposits were composed of neoplastic cells in trabeculae, solid sheets, or a pseudopapillary arrangement. The tumor in case 5 contained multiple foci of eosinophilic hyaline globules **Image 4**. These hyaline globules did not stain for collagen IV (data not shown). Psammoma bodies were not identified in any of the examined tumors.

Immunohistochemical evaluation **Table 2** revealed no staining with cytokeratin markers, including AE3, AE1, pankeratin, CK7, and ker34βE12. Tumor cells were also negative

for HMB45, SMA, LCA (CD45), and calretinin. The tumor cells were focally positive for vimentin **Image 5A** and diffusely positive for CD10 **Image 5B**. Strong nuclear expression of TFE3 occurred in approximately 80% of the cells from each tumor **Image 6**. The amount of staining was relatively constant and did not vary between tumors with different nuclear grades or between areas with different architectural patterns.

Electron microscopy demonstrated abundant lipid droplets and glycogen, similar to clear cell RCC, and occasional granules vaguely resembling those seen in alveolar soft part sarcoma **Image 7**.

Diagnosis

In view of the positive stain for TFE3, all patients were diagnosed with translocation RCC of the TFE3 type based on the primary tumor (cases 1 and 3-5) or metastases (case 2). Based on TNM status, all cases were classified as clinical stage IV.¹²

Discussion

RCCs associated with *TFE3* gene fusions are relatively rare tumors predominantly diagnosed in children.¹ It is estimated that approximately one third of pediatric renal carcinomas are *TFE3*-related translocation carcinomas,¹³ whereas clear cell RCCs make up 15% of renal carcinomas in children.^{14,15} Unlike in children, clear cell RCCs make up 70% of renal carcinomas in adults and 53% in young adults,¹⁵ but the

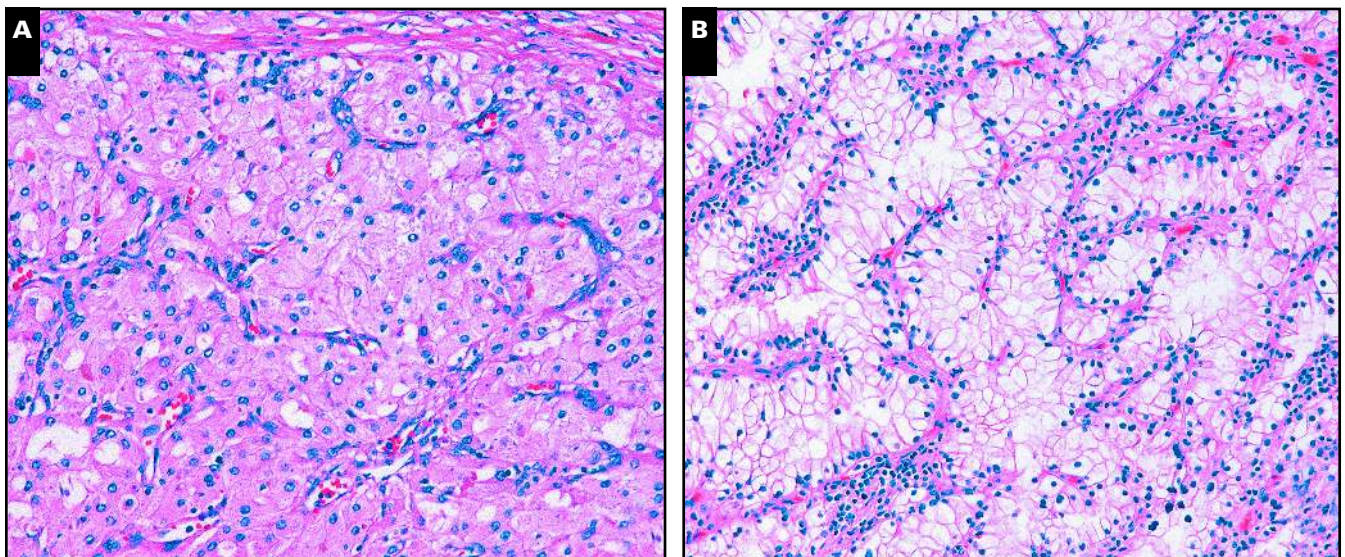


Image 2 Neoplastic cells containing granular eosinophilic cytoplasm (**A**, Case 5) and clear cytoplasm (**B**, Case 3). Lymphocytes were present in the tumor in case 3 (**A** and **B**, H&E, ×400).

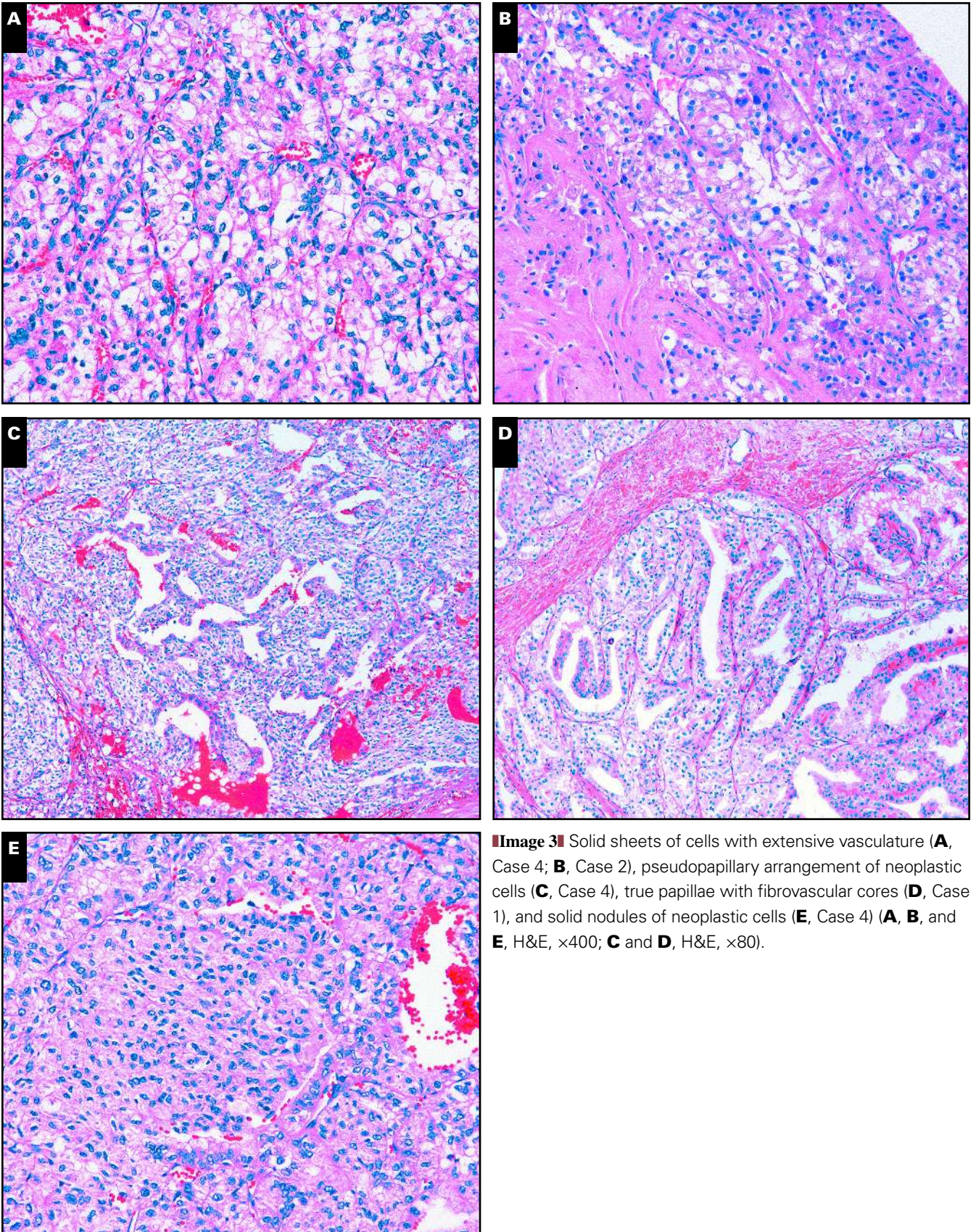


Image 3 ■ Solid sheets of cells with extensive vasculature (**A**, Case 4; **B**, Case 2), pseudopapillary arrangement of neoplastic cells (**C**, Case 4), true papillae with fibrovascular cores (**D**, Case 1), and solid nodules of neoplastic cells (**E**, Case 4) (**A**, **B**, and **E**, H&E, ×400; **C** and **D**, H&E, ×80).

Downloaded from <https://academic.oup.com/ajcp/article/128/1/70/1759868> by guest on 20 August 2022

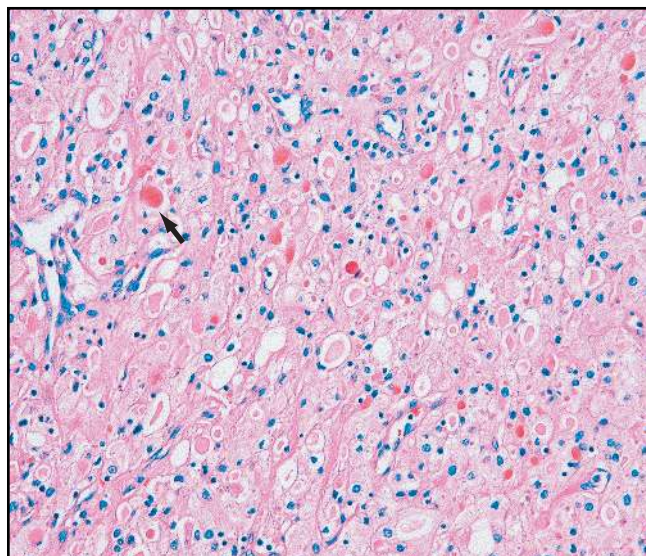


Image 4 (Case 5) Eosinophilic hyaline globule (arrow) similar to the basement membrane aggregates seen in translocation renal cell carcinomas associated with TFE3 (H&E, $\times 400$).

Table 2
Immunohistochemical Results for Five Cases of Renal Cell Carcinoma Associated With Xp11.2

Marker	Result
TFE3	Positive
AE1	Negative
AE3	Negative
Cytokeratin 7	Negative
Pankeratin	Negative
Ker34 β E12	Negative
Vimentin	Focally positive
Smooth muscle actin	Negative
CD45	Negative*
CD10	Diffusely positive
HMB45	Negative
Calretinin	Negative

* Lymphocytes within the tumor were positive.

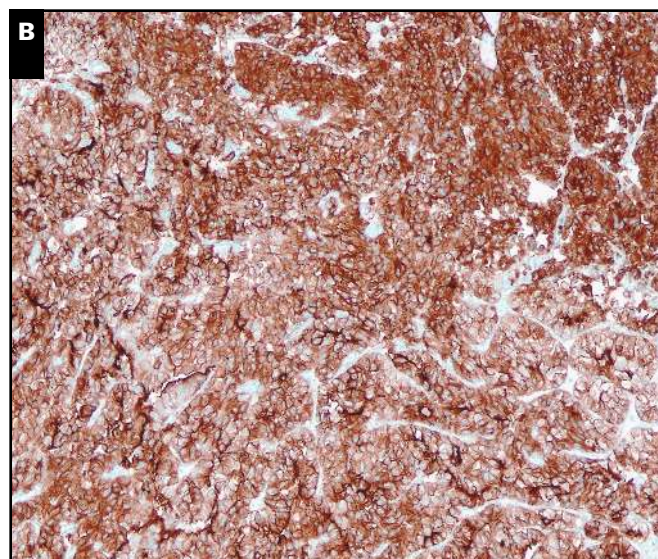
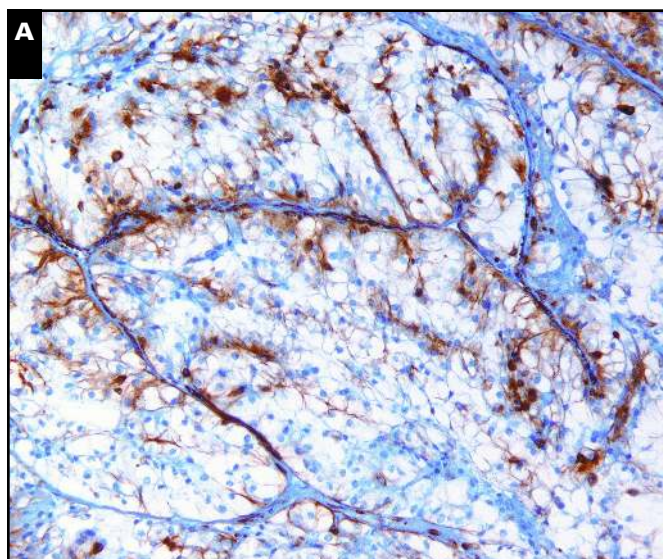


Image 5 Neoplastic cells were focally positive for vimentin (**A**) and diffusely positive for CD10 (**B**) (**A** and **B**, $\times 400$).

incidence of *TFE3* translocation carcinomas in these age groups is not known. The cases reported herein indicate that translocation RCCs also occur in adults (mean age, 32.6 years; oldest, 41 years) and are more aggressive and manifest at a higher clinical stage than in pediatric patients.

In contrast with clear cell RCCs, *TFE3*-related renal carcinomas were originally reported to have papillary architecture.^{16,17} Only 1 of the cases reported herein had this feature. In fact, there was enough morphologic overlap between these tumors and clear cell RCC that a diagnosis

based only on H&E-stained sections could not be made. Immunohistochemical analysis revealed lack of staining with cytokeratin antibodies, as expected for *TFE3* renal carcinomas.¹ Similar to clear cell carcinomas, these tumors were focally positive with vimentin and strongly positive with CD10. The only consistent and reliable diagnostic feature was nuclear staining with anti-*TFE3* antibodies. The difficulty in distinguishing between clear cell RCCs and *TFE3* translocation carcinomas supports the need for detecting *TFE3* mutations in renal carcinomas.

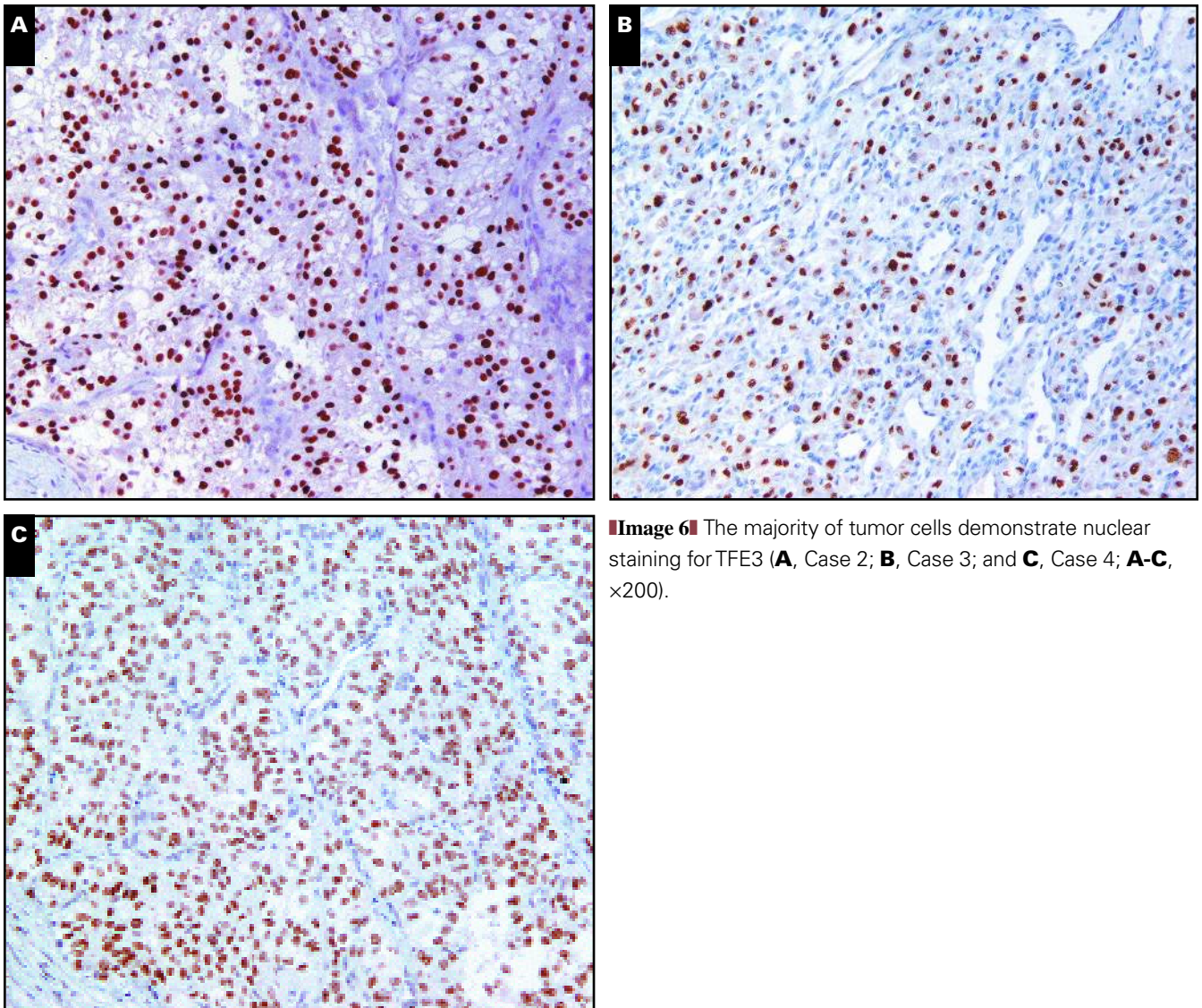


Image 6 The majority of tumor cells demonstrate nuclear staining for TFE3 (**A**, Case 2; **B**, Case 3; and **C**, Case 4; **A-C**, $\times 200$).

The initial complaints of the patients described herein were nonspecific, their medical histories were not significant, and none had previous hazardous exposures or chemotherapy. The lack of exposure to chemotherapy is significant considering that chemotherapy in childhood is a risk factor for developing translocation RCCs.¹⁸ Despite the innocuous initial complaints and the lack of significant history, all patients were diagnosed initially with clinical stage IV disease owing to distant metastases (M1) or multiple lymph node metastases (N2) (Table 1). A variety of therapeutic interventions were tried, but most tumors followed a rapidly progressive course with a mean life expectancy of 18 months following diagnosis. The rapid course of translocation RCC in these cases belies the previous contention that these tumors are indolent.¹ It is interesting that rare pediatric translocation RCCs with aggressive behavior have recently been reported.^{19,20} These aggressive pediatric tumors were associated with distant metastases,

similar to the adult cases reported herein, whereas indolent *TFE3* translocation carcinomas were only associated with lymph node involvement.

It is possible that translocation RCCs developed when our patients were young but were not detected until reaching an advanced stage. With this hypothesis, the overall life span of adults with rapidly terminal disease and pediatric patients with slower disease courses would be similar. Another possibility is that translocation RCC is more aggressive when it occurs in adults than when it occurs in children. In the latter scenario, the majority of translocation RCCs in adults would have been misdiagnosed if testing for the *TFE3* mutation had not been performed. Consistent use of antibodies against TFE3 in all RCCs, regardless of patient age, may be necessary to determine the true incidence of this tumor. It may also reveal 2 peaks of translocation RCC: an indolent neoplasm in children and an aggressive neoplasm in adults.

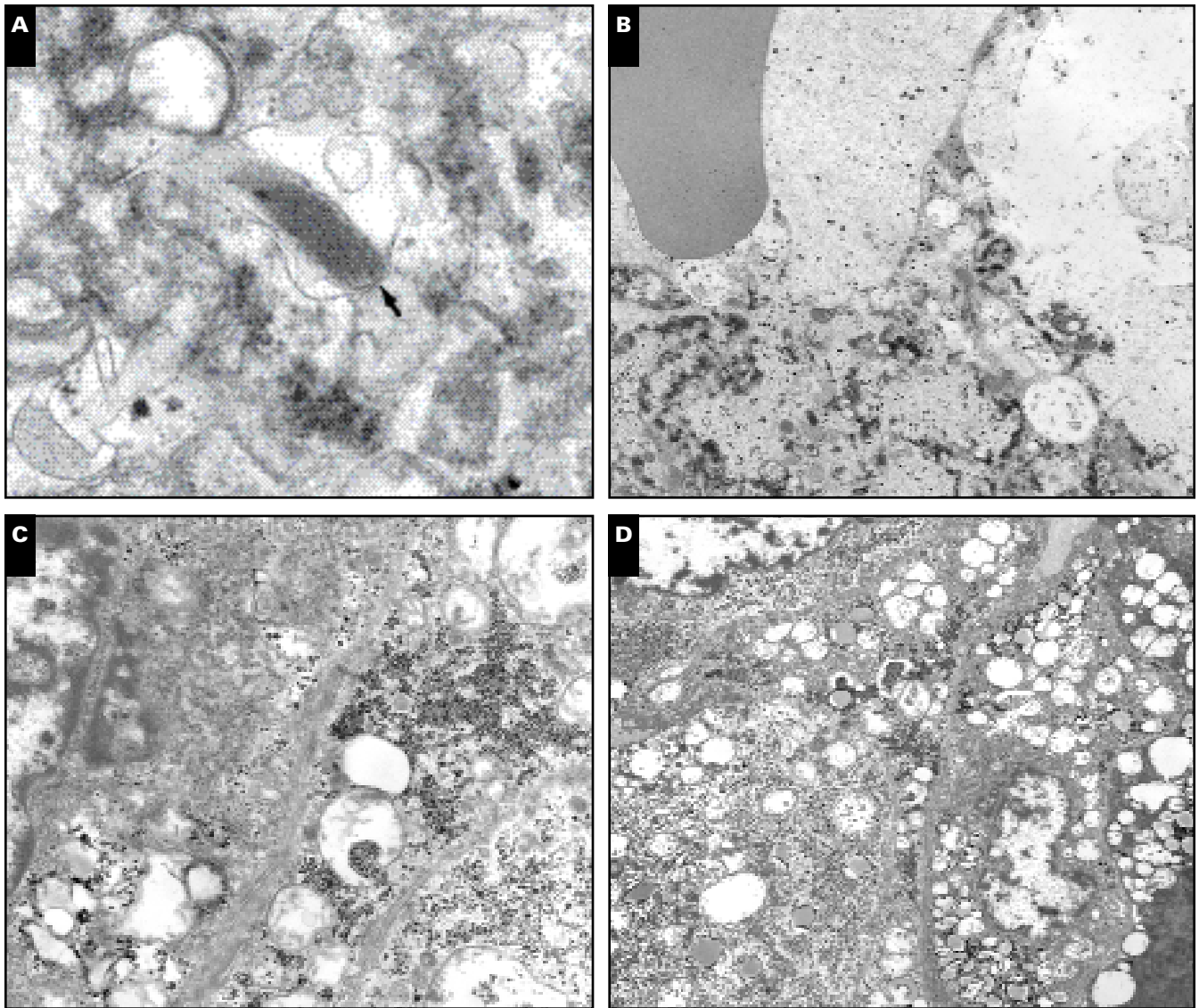


Image 7 Ultrastructural analysis revealed abundant lipid droplets and glycogen similar to clear cell renal cell carcinoma (**B, C**, and **D**). Rare rhomboid crystals (**A**, arrow), similar to alveolar soft part sarcoma, were identified (**A**, $\times 12,000$; **B**, $\times 3,000$; **C**, $\times 4,400$; **D**, $\times 3,000$).

RCCs involving mutations of the *TFE3* or *TFEB* gene might be classified together as *MiTF/TFE* renal translocation carcinomas.^{19,21} *MiTF* is required for melanocyte differentiation.²² *MiTF* and *TFEB* are known to interact as heterodimers in binding DNA sequences⁵ and may be involved in regulating specific melanocyte differentiation genes. Although *TFE3* also has the ability to form heterodimers with *MiTF*, the ability to bind promoters necessary for the regulation of melanocyte differentiation seems to be hindered.²³ This discrepancy between the binding ability of *TFEB* heterodimers compared with *TFE3* heterodimers may explain why RCCs with mutations of *TFEB* express HMB45 and *TFE3*-associated RCCs do not.⁷

Morphologic similarities on H&E-stained slides between published cases of *TFEB*-related RCCs and *TFE3*-related

RCCs in the present study support the notion of combining the tumors into a single category. *TFEB*-associated RCCs have distinct aggregates of eosinophilic basement membrane material.⁷ The tumor from 1 patient in the present study (case 5) contained multiple foci of eosinophilic hyaline globules; however, these globules did not contain collagen IV, suggesting that they were not composed of basement membrane-type material. This tumor was further examined and found to be negative for *TFEB* expression by immunohistochemical analysis (data not shown).

The cases reported herein show that translocation RCCs involving *TFE3* can occur in adults. In adults, unlike in children, these tumors have an aggressive clinical course, and H&E morphologic examination alone is not reliable for

differentiation between clear cell–type and translocation-type neoplasms. More widespread use of immunohistochemical stains for TFE3 is, therefore, warranted.

From the Departments of ¹Pathology, ²Hematology-Oncology, and ³Urology, Loyola University Medical Center, Maywood, IL.

Address reprint requests to Dr Picken: Dept of Pathology, Bldg 110, Rm 2242, Loyola University Medical Center, 2160 S First Ave, Maywood, IL 60153; mpicken@lumc.edu.

References

- Argani P, Ladanyi M. Renal carcinomas associated with Xp11.2 translocations/TFE3 gene fusions. In: Eble JN, Sauter G, Epstein JI, et al, eds. *Pathology and Genetics of Tumours of the Urinary System and Male Genital Organs*. Lyon, France: IARC Press; 2004:37-38. *World Health Organization Classification of Tumours*.
- Picken MM. The evolving concept of renal neoplasia: impact of emerging molecular and electron microscopic studies. *Ultrastruct Pathol*. 2005;29:277-282.
- Tonk V, Wilson KS, Timmons CF, et al. Renal cell carcinoma with translocation (X;1): further evidence for a cytogenetically defined subtype. *Cancer Genet Cytogenet*. 1995;81:72-75.
- Argani P, Antonescu CR, Illei PB, et al. Primary renal neoplasms with the ASPL-TFE3 gene fusion of alveolar soft part sarcoma: a distinctive tumor entity previously included among renal cell carcinomas of children and adolescents. *Am J Pathol*. 2001;159:179-192.
- Hemesath TJ, Steingrimsson E, McGill G, et al. Microphthalmia, a critical factor in melanocyte development, defines a discrete transcription factor family. *Genes Dev*. 1994;8:2770-2780.
- Beckmann H, Su LK, Kadesch T. TFE3: a helix-loop-helix protein that activates transcription through the immunoglobulin enhancer muE3 motif. *Genes Dev*. 1990;4:167-179.
- Argani P, Hawkins A, Griffin CA, et al. A distinctive pediatric renal neoplasm characterized by epithelioid morphology, basement membrane production, focal HMB45 immunoreactivity, and t(6;11)(p21.1;q12) chromosome translocation. *Am J Pathol*. 2001;158:2089-2096.
- Weternan MA, Wilbrink M, Geurts van Kessel A. Fusion of the transcription factor TFE3 gene to a novel gene, PRCC, in t(X;1)(p11;q21)-positive papillary renal cell carcinomas. *Proc Natl Acad Sci U S A*. 1996;93:15294-15298.
- Clark J, Lu YJ, Sidhar SK, et al. Fusion of splicing factor genes PSF and NonO (p54nrp) to the TFE3 gene in papillary renal cell carcinoma. *Oncogene*. 1997;15:2233-2239.
- Argani P, Antonescu CR, Couturier J, et al. PRCC-TFE3 renal carcinomas: morphologic, immunohistochemical, ultrastructural, and molecular analysis of an entity associated with the t(X;1)(p11.2;q21). *Am J Surg Pathol*. 2002;26:1553-1566.
- Picken MM, Curry JL, Lindgren V, et al. Metanephric adenocarcinoma in a young adult: morphologic, immunophenotypic, ultrastructural, and fluorescence in situ hybridization analyses: a case report and review of the literature. *Am J Surg Pathol*. 2001;25:1451-1457.
- Greene FL, Page DL, Fleming ID, et al. *AJCC Cancer Staging Handbook*. 6th ed. New York, NY: Springer; 2002.
- Argani P, Ladanyi M. Translocation carcinomas of the kidney. *Clin Lab Med*. 2005;25:363-378.
- Bruder E, Passera O, Harms D, et al. Morphologic and molecular characterization of renal cell carcinoma in children and young adults. *Am J Surg Pathol*. 2004;28:1117-1132.
- Cao Y, Paner GP, Perry KT, et al. Renal neoplasms in younger adults: analysis of 112 tumors from a single institution according to the new 2004 World Health Organization classification and 2002 American Joint Committee on Cancer Staging System. *Arch Pathol Lab Med*. 2005;129:487-491.
- Tomlinson GE, Nisen PD, Timmons CF, et al. Cytogenetics of a renal cell carcinoma in a 17-month-old child: evidence for Xp11.2 as a recurring breakpoint. *Cancer Genet Cytogenet*. 1991;57:11-17.
- Meloni AM, Sandberg AA, Pontes JE, et al. Translocation (X;1)(p11.2;q21): a subtype of renal adenocarcinomas [letter]. *Cancer Genet Cytogenet*. 1992;63:100-101.
- Argani P, Lae M, Ballard ET, et al. Translocation carcinomas of the kidney after chemotherapy in childhood. *J Clin Oncol*. 2006;24:1529-1534.
- Argani P. The evolving story of renal translocation carcinomas. *Am J Clin Pathol*. 2006;126:332-334.
- Ramphal R, Pappo A, Zielenska M, et al. Pediatric renal cell carcinoma: clinical, pathologic, and molecular abnormalities associated with the members of the mit transcription factor family. *Am J Clin Pathol*. 2006;126:349-364.
- Argani P, Ladanyi M. Distinctive neoplasms characterized by specific chromosomal translocations comprise a significant proportion of paediatric renal cell carcinomas. *Pathology*. 2003;35:492-498.
- Bertolotto C, Abbe P, Hemesath TJ, et al. Microphthalmia gene product as a signal transducer in cAMP-induced differentiation of melanocytes. *J Cell Biol*. 1998;142:827-835.
- Verastegui C, Bertolotto C, Bille K, et al. TFE3, a transcription factor homologous to microphthalmia, is a potential transcriptional activator of tyrosinase and *Tyrp1* genes. *Mol Endocrinol*. 2000;14:449-456.